

Detection of the translational oscillations of the Earth's solid inner core based on the international superconducting gravimeter observations

SUN Heping¹, XU Jianqiao¹ & B. Ducarme²

1. Key Laboratory of Geodynamic Geodesy, Institute of Geodesy and Geophysics, Chinese Academy of Sciences, Wuhan 430077, China;
 2. Royal Observatory of Belgium, Belgium National Fund for Scientific Research, Av. Circulaire 3, B-1180, Brussels, Belgium
- Correspondence should be addressed to Sun Heping
(e-mail: heping@asch.whigg.ac.cn)

Abstract Based on the 21 series of the high precision tidal gravity observations recorded using superconducting gravimeters (SG) at 14 stations distributed globally (in totally about 86 years), the translational oscillations of the Earth's solid inner core (ESIC) is detected in this paper. All observations are divided into two groups with G-I group (8 relatively longer observational series) and G-II group (13 relatively shorter observational series). The detailed corrections to minute original observations for each station are carried out, the error data due to the earthquakes, power supply impulses and some perturbations as change in atmospheric pressure and so on are carefully deleted for the first step, the gravity residuals are obtained after removing further synthetic tidal gravity signals. The Fast Fourier Transform analysis is carried out for each residual series, the estimations of the product spectral densities in the sub-tidal band are obtained by using a multi-station stacking technique. The 8 common peaks are found after further removing the remaining frequency dependent pressure signals. The eigenperiods, quality factors and resonant strengths for these peaks are simulated. The numerical results show that the discrepancies of the eigenperiods for 3 of 8 peaks, compared to those of theoretical computation given by Smith, are only 0.4%, -0.4% and 1.0%. This coincidence signifies that the dynamical phenomenon of the Earth's solid inner core can be detected by using high precision ground gravity observations. The reliability of the numerical computation is also checked, the spectral peak splitting phenomenon induced by Earth's rotation and ellipticity is preliminary discussed in this paper.

Keywords: observations of global superconducting gravimeters, estimation of the product spectral density, translational oscillations of the solid inner core, determination of the resonance parameters.

DOI: 10.1360/03wd0242

Before about 100 years, the layered structures of the Earth's body and the existence of the liquid core had been found, then the solid inner core and detailed structures in the interior of the Earth are demonstrated, it proves that the satisfied achievements had been obtained in recogni-

tion of the Earth's interior structures. In recent years, with the increasing requirements of the basic sciences and space techniques to geodynamics of the Earth's interior, the theoretical study and practical detection of the geodynamic phenomena of the liquid core and of the translational oscillations of the ESIC are now more and more important^[1,2]. The researches on the geodynamic problem of the liquid core have obtained great progress, however, only some valuable attempts are carried out for study in the translational oscillations of the ESIC, there are still not a well accepted theoretical model and complete detection result until nowadays^[3]. The past researches have shown that the gravity measurement is a unique effective method in the study of the Earth's interior structure and geodynamical phenomena, differing from seismological technique^[4]. The new prospects and hopes in the study and detection of the translational oscillations of the ESIC emerge thanks to the successful construction of the new high precision SG in the early of 1980s in GWR company in USA, and the accumulation of data sets in an international network. The researches have shown that it is hopeful for the mankind to recognize correctly the characteristics for the detailed structure and density distribution at the boundary of the Earth's liquid outer core and solid inner core by determining accurately the parameters of the translational oscillations of the ESIC^[5,6].

The translational oscillations of the ESIC at its equilibrium position are the fundamental free modes in the dynamical problems of the Earth's interior, which include usually three parts, i.e., the movement at Earth's rotation axis, the equatorial prograde and equatorial retrograde translational movements^[1,7]. For a sphere symmetrical, layered and non-rotating Earth model, these spheroidal normal modes are usually described by using degree 1 spheroidal displacement vectors. The modes of the translational oscillations are also called the Slichter modes since they are found by Slichter for the first time. By using a generalized spherical harmonic expansion of the movement equation for a rotational and slight ellipticity Earth model, the translational oscillations of the ESIC were theoretically studied by Smith, the eigen-function solutions of the spheroidal displacement vectors were given in his study. The predominant components of these eigenmodes are expressed with spheroidal σ_1^m and toroidal τ_2^m displacements, the truncation form of the solutions are described by using spherical harmonic developments with order and degree (1, m) and (2, m) in form as $s^m = \sigma_1^m + \tau_2^m$, where $m = -1, 0, 1$ represent respectively the equatorial prograde, axis, and equatorial retrograde translational modes. Based on a DG597 Earth model, the eigenperiods were calculated, the corresponding studies have emerged that the influence of the stratification in fluid outer core and the elastic property of the solid inner

core on eigenperiods to be significant^[8]. The numerical computations based on theory also showed that the gravity variation signal is at $2 \times 10^{-11} \text{ m/s}^2$ level due to the equatorial retrograde translational mode during the Chile Earthquake in 1960. Since the existence of the Earth's rotation, the infinite couplings among the spheroidal and toroidal vectors in displacement eigenfunction due to the action of Coriolis force appear, hence it is very difficult to evaluate accurately the truncation errors. To overcome this uncertainty due to the convergence of the generalized spherical harmonic expansion, the theoretical studies were developed by Smylie using a finite element technique based on so-called "subseismic approximation". The parameters of the translational oscillations differing from those of Smith were obtained for Earth's model CORE11 and 1066A^[5].

In recent years, many valuable attempts are carried out by international colleagues in detection of the dynamic phenomena of the liquid core and solid inner core. By using Strasbourg SG data, Hinderer had studied the existence of the Slichter modes^[9]. Based on the Brussels SG observations, the inertial oscillation modes of the liquid outer core provoked by the Hindu Kush deep large earthquake on December 30, 1983 were studied by Melchior and Ducarme^[4]. With the IDA gravity observations, the existence of the modes in Earth's liquid core was also checked by Cummins^[10]. The translational modes were obtained by Smylie et al. using 4 ground based SG observations in Europe^[11] and also the translation oscillations of the ESIC were confirmed late on by Courtier et al. using more SG observations^[12]. The free core nutation problem of the Earth's liquid core has been studied by Sun et al. and Xu et al. based on the global distributed SG observations^[13,14], after that, Sun et al. constructed also the most recent Earth tidal experimental models^[15]. However, due to its complicated problem, there exist significant discrepancies between theoretical prediction and real detection.

With the rapid progress of the electronic technique, especially the successful construction of the high precision SG and its wide use globally, the reliable assurance is now provided us for obtaining the small variation of the gravity on the surface of the Earth induced by the dynamics of the Earth's deep interior^[16]. Many excellent characteristics of the SG emerge due to overcoming the shortcomings as serious instrument drift and unstable in long period observations when using a spring gravimeter, as extremely wide dynamical linear frequency property and measuring range (from second to years), extreme high measuring accuracy (at 10^{-11} m/s^2 level) and extremely stable yearly drift (10^{-8} m/s^2 level)^[17,18]. In our study, the phenomena of the translational oscillations of the ESIC will be investigated by using the SG data from a global network in order to do necessary attempt and to establish a preliminary basis for further theoretical study and practical detection,

and also to provide the valuable reference information for studying the physical properties in the Earth's deep interior.

1 Data preparation

The SG observation periods used in present researches are listed in Table 1, in total there are 14 stations and 21 observation series. In order to study and compare conveniently, the data sets from all stations are divided into two groups, i.e., (1) G-I group, mainly including 8 relatively longer series recorded with old GWR instruments, the observations are mainly located in the periods from 1982 to 2000, and (2) G-II group, mainly including 13 relatively shorter series recorded with new GWR instruments, the observations are mainly located in the Global Geodynamics Project (GGP) periods after July, 1997. The SG instruments with identical model, the same digital data acquisition system, filters and data sampling rate are accepted for all participated members in the GGP. There are 7 stations in Europe as Brussels, Mernback, Metsahovi, Potsdam, Strasbourg, Vienne and Wetzell, 3 stations in Asia as Esashi, Matsushiro and Wuhan, 2 stations in North America as Boulder and Cantley, and 2 stations in the Southern Hemisphere as Canberra and Syowa.

It is an important basic work in this study for the detailed preprocessing of the original observations. The Tsoft preprocessing package recommended by the International Center for Earth Tides are used^[19]. By using a relatively strong man-machine interface, the abnormal signals as jumps due to instrument, spikes caused by power impulse and error data due to seismological activities and so on are carefully eliminated for both minute sampling gravity and station pressure obtained via international data exchange channel. The short-term interruptions in data recordings induced by the earthquakes, refilling liquid helium and stop of the power supply are filled using the spline interpolation^[20-22]. By using an identical filter for each station, the hourly data of the tidal gravity and station pressure are arranged based on the minute samplings^[23]. Considering the gravity signals induced by the translational oscillations of the ESIC are usually located on the sub-tidal band, i.e., at the period less than 8 h, it is necessary for us to remove further tidal gravity, atmospheric pressure and instrument drift^[24,25]. Then the gravity observation residuals $\text{Res}(t)$ are obtained, the fitting formula is given as follows^[26]:

$$\begin{aligned} \text{Res}(t) = & \text{Obs}(t) - \sum_k \delta_k \sum_{i=\alpha_k}^{\beta_k} A_i \cos(\omega_i t + \varphi_i + \Delta\varphi_k) \\ & - C \cdot \text{Pr}(t) - \sum_{i=0}^2 a_i \cdot t^i, \end{aligned} \quad (1)$$

where $\text{Obs}(t)$ and $\text{Pr}(t)$ represent the original gravity observation and pressure variation at time t , respectively. δ_k and $\Delta\varphi_k$ are the unknown amplitude factor and phase lag

for the k th tidal wave group, α_k and β_k the starting and ending arguments of the k th tidal wave group in the tidal generating potential table, A_i , ω_i and φ_i the theoretical amplitude, angle frequency and preliminary phase. C is the atmospheric gravity regression coefficient. The 4th term in right side of eq. (1) represents the instrument drift of the second order polynomial, a_i is the unknown coefficients. By using synthetic signal composed with high precision celestial catalogue given by Merriam, the atmospheric gravity admittances C and fitting coefficients of the instrumental drift a_i are obtained using a least square fitting, the corresponding results are listed in Table 1. Figs. 1 and 2 demonstrate the gravity observational residual series for both groups G- I and G- II. It is found that there exists an obvious polar gravity effect in gravity residuals, and the analysis demonstrates that the residual amplitude reflects the station background noise level. The relatively large residuals for stations Cantly and Wuhan in G- I group and Vienna and Matsushiro in G- II group are clearly seen in Figs. 1 and 2, it signifies that these data are more greatly influenced by station background noise and local perturbations than the data obtained from other stations.

2 Residual power spectral density and product spectral density

Based on the accumulated experiences in numerical computation given by Smylie, for certain observation series of the gravity residual and pressure, the averaging spectral analysis technique for each data block is used in

order to obtain reliability of the power spectral density with high resolution^[11]. The selected data block length is given as $M = 12000$ h, there exists the overlapping of 75% for two neighboring data blocks. If the whole data length is T , then the number of the data blocks κ can be given as

$$\kappa = 4 \frac{T}{M} - 3, \quad (2)$$

then the Fourier spectrum $F(n; \omega)$ for n th data block is then given as

$$F(n; \omega) = \int_{-\infty}^{+\infty} \text{Res}(t) \cdot w(t) \cdot e^{-i\omega t} dt, \quad (3)$$

where ω is the angle frequency, $w(t)$ the window function. The Parzen window with length M is selected in this computation. Averaging the results for the κ data blocks, then the Fourier spectrum for the whole data series can be obtained as

$$F(\omega) = \frac{1}{\kappa} \sum_{n=1}^{\kappa} F(n; \omega) = \tilde{A}(\omega) \cdot e^{i\tilde{\varphi}(\omega)}, \quad (4)$$

where $\tilde{A}(\omega)$ and $\tilde{\varphi}(\omega)$ are the amplitude and phase. Then the Fourier power spectral density for this series can be given as

$$\tilde{P}(\omega) = F^*(\omega) \cdot F(\omega) / I = \tilde{A}^2(\omega) / I, \quad (5)$$

where I is a normalization factor given by

$$I = \int_{-M/2}^{M/2} w^2(t) dt. \quad (6)$$

When using N observation series, the Fourier spec-

Table 1 Global SG observation period, atmospheric gravity admittance and fitting parameters of the instrument drift

Station	Observation period	$C/\text{nm} \cdot \text{s}^{-2} \cdot \text{hPa}^{-1}$	$a_0/\text{nm} \cdot \text{s}^{-2}$	$a_1/\text{nm} \cdot \text{s}^{-2}$	$a_2/\text{nm} \cdot \text{s}^{-2}$
G- I group					
Brussels1/Belgium	1982-06-02—1986-10-15	-3.428	5477.74	5.1615×10^{-3}	-2.27187×10^{-7}
Brussels2/ Belgium	1986-11-15—2000-09-20	-3.428	8261.31	-4.33364×10^{-3}	3.95268×10^{-8}
Boulder/USA	1995-04-12—2001-03-29	-3.240	4100.57	1.21226×10^{-2}	-6.78259×10^{-8}
Cantley/Canada	1989-11-07—1993-08-17	-3.000	-1416.08	-2.57169×10^{-1}	2.18132×10^{-6}
Membach/Belgium	1995-08-04—2000-05-31	-3.428	-1068.06	8.6815×10^{-3}	-7.62658×10^{-8}
Potsdam/Germany	1992-06-30—1998-10-08	-3.500	42.6904	1.29067×10^{-2}	-1.25675×10^{-7}
Strasbourg/France	1987-07-11—1996-06-25	-3.000	-752.296	3.76773×10^{-2}	-3.09172×10^{-7}
Wuhan/China	1988-11-17—1994-01-04	-3.840	-270.722	7.53626×10^{-3}	-4.17849×10^{-7}
G- II group					
Brussels/ Belgium	1997-07-01—2000-09-21	-3.428	8065.87	1.43421×10^{-2}	-3.33212×10^{-8}
Boulder/USA	1997-07-01—2001-03-09	-3.240	4298.51	1.19642×10^{-2}	-1.44745×10^{-7}
Cantley/Canada	1997-07-01—1999-09-30	-3.000	-530.54	7.0119×10^{-3}	-3.58618×10^{-7}
Canberra/Australia	1997-07-01—1999-12-31	-3.002	3271.41	3.45377×10^{-3}	-6.42189×10^{-9}
Membach/Belgium	1997-07-01—2000-05-31	-3.428	-909.798	-4.94036×10^{-6}	1.37124×10^{-7}
Metsahovi/Finland	1997-07-01—2000-06-30	-3.810	-1854.78	2.89513×10^{-2}	-2.69912×10^{-7}
Esashi/Japan	1997-07-01—1999-12-31	-3.145	3161.77	-3.04659×10^{-3}	2.58302×10^{-7}
Matsushiro/Japan	1997-07-01—1999-12-31	-3.334	2334.66	4.6403×10^{-2}	-4.85485×10^{-7}
Strasbourg/France	1997-07-01—1999-07-31	-3.000	2.56017	1.53173×10^{-3}	3.06189×10^{-8}
Syowa/ Antarctic	1997-07-01—1998-12-31	-3.920	-1914.72	-8.69446×10^{-3}	-2.89515×10^{-7}
Vienna/Austria	1997-07-01—1999-06-30	-3.220	-4995.73	4.39883×10^{-3}	-1.24985×10^{-7}
Wetzell/Germany	1996-07-28—1998-09-23	-3.484	2353.82	-2.8184×10^{-1}	-3.79209×10^{-7}
Wuhan/China	1997-12-20—2000-08-31	-3.498	3111.63	4.89498×10^{-3}	-1.43076×10^{-7}

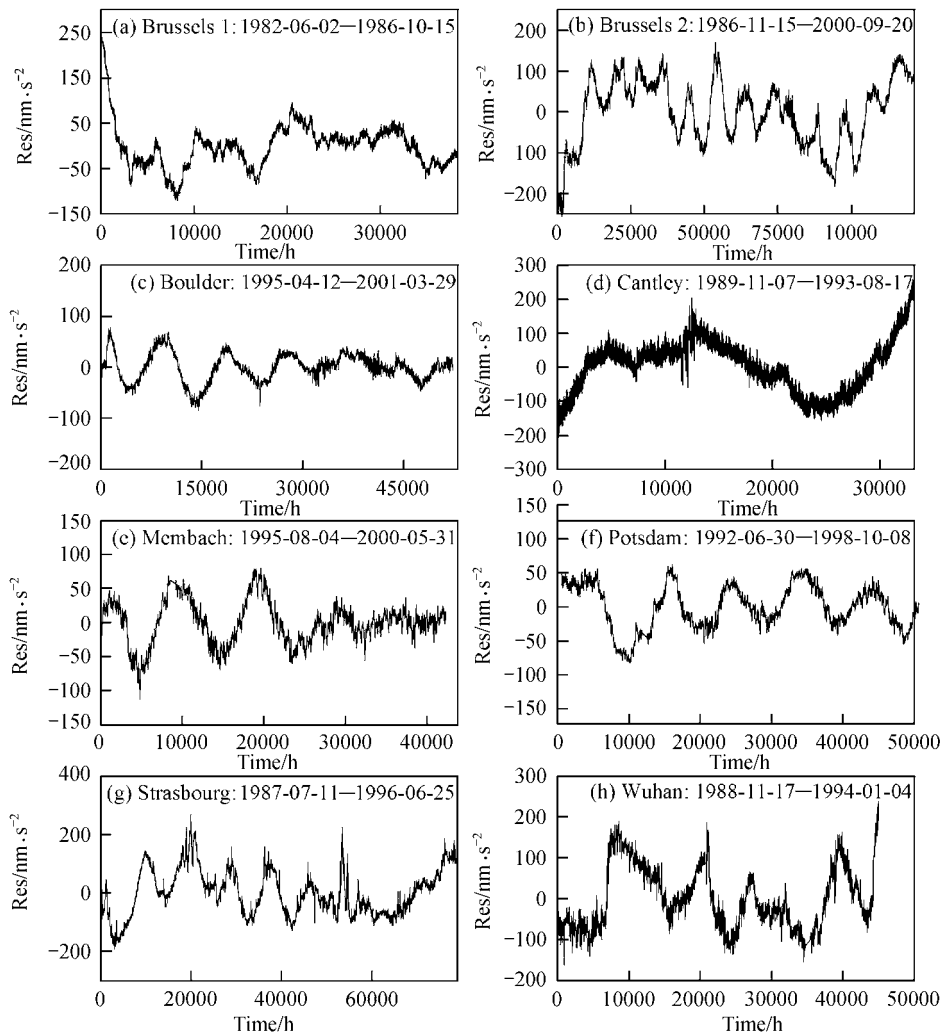


Fig. 1. SG observation residuals for stations in G- I group.

trum and power spectral density are represented as $F_i(\omega)$ and $\tilde{P}_i(\omega)$ ($i = 1, 2, \dots, N$ are the series number), the product spectral density (PSD) estimation $\bar{P}(\omega)$ can then be obtained by [11]

$$\bar{P}(\omega) = \left[\prod_{i=1}^N \tilde{P}_i(\omega) \right]^{\frac{1}{N}} = \left\{ \prod_{i=1}^N \left[F_i^*(\omega) \cdot F_i(\omega) / I \right] \right\}^{\frac{1}{N}}. \quad (7)$$

3 Numerical results and discussions

Based on eq. (5), the evaluations of the Fourier power spectral density for both gravity residual and pressure in G-I and G-II groups are obtained (Figs. 3 and 4). By using a multi-station data stacking formula given in eq. (7), their PSD estimation at sub-tidal band is also obtained (Figs. 5 and 6). It is found that though the pressure corrections are carried out for each gravity series, there exist still significant S5 and S6 peaks in the PSD estima-

tions that relate obviously to the solar heating. The study shows also that there exists the characteristic of the frequency dependence for the influence of the pressure on gravity field [24]. Therefore, it is far away from removing completely the pressure effect from gravity observation when using only single admittance determined by a least square fitting technique in time domain. Since such a single regression coefficient has an averaging property in the whole frequency band. Therefore, it is necessary for us to further consider the frequency dependence of the pressure on gravity influence, in order that some weak geodynamical signals in Earth's deep interior can emerge in the surface gravity observations.

In order to further improve effectively the signal-noise level, the frequency-dependent 3 order polynomials are used to delete the remaining pressure components in the PSD results. The fitting process of the background noise $Bn(f)$ for pressure and gravity in the PSD

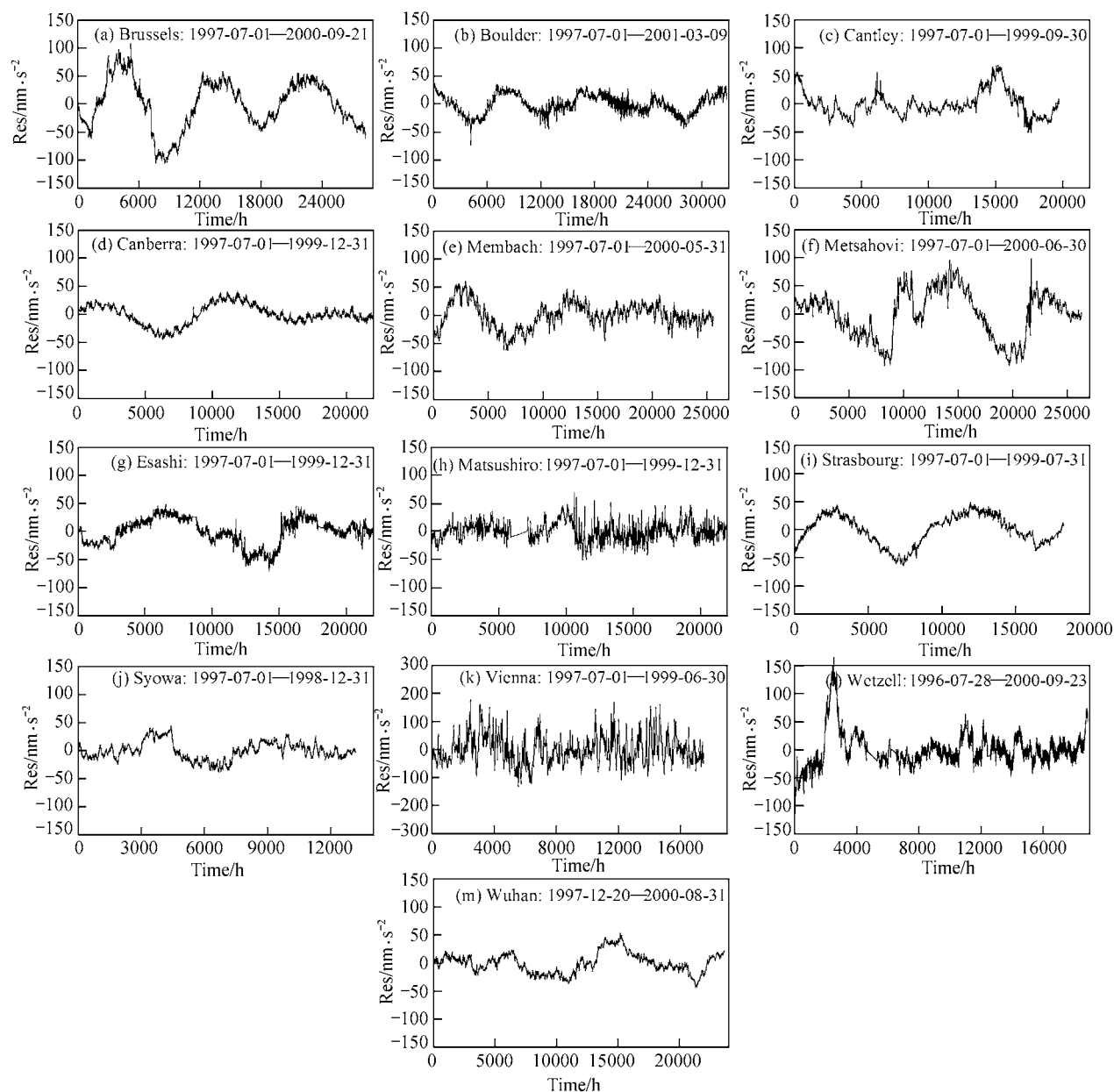


Fig. 2. SG observation residuals for stations in G-II group.

results is simulated. The formula is given as

$$Bn(f) = b_0 + b_1 \cdot f + b_2 \cdot f^2 + b_3 \cdot f^3, \quad (8)$$

where b_0 , b_1 , b_2 and b_3 are the unknown constants in the fitting polynomials. The energy ratios of the gravity and pressure in the PSD estimations for S5 and S6 are taken as the correction coefficients of the pressure signals at this band. The pressure correction coefficients in other subtidal band are obtained by using a frequency-dependent linear interpolation technique. Then the remaining pressure signals are finally removed from the gravity PSD estimations. Fig. 7 gives the final PSD results of the grav-

ity residuals after removing the remaining pressure signals for both G-I and G-II groups.

It is found from Fig. 7 that the averaging background noise of the gravity residuals in G-II group (lower plot) is lower than that given in G-I group (upper plot). This signifies that the quality of the SG observations is improved significantly in the GGP period. It seems that no signals from core modes at a period of (3.58 h (0.227 cpd), 3.76 h (0.266 cpd) and 4.01 h (0.249 cpd)) claimed by Smylie and Courtier are found in our final PSD results for both G-I and G-II groups. However, several significant

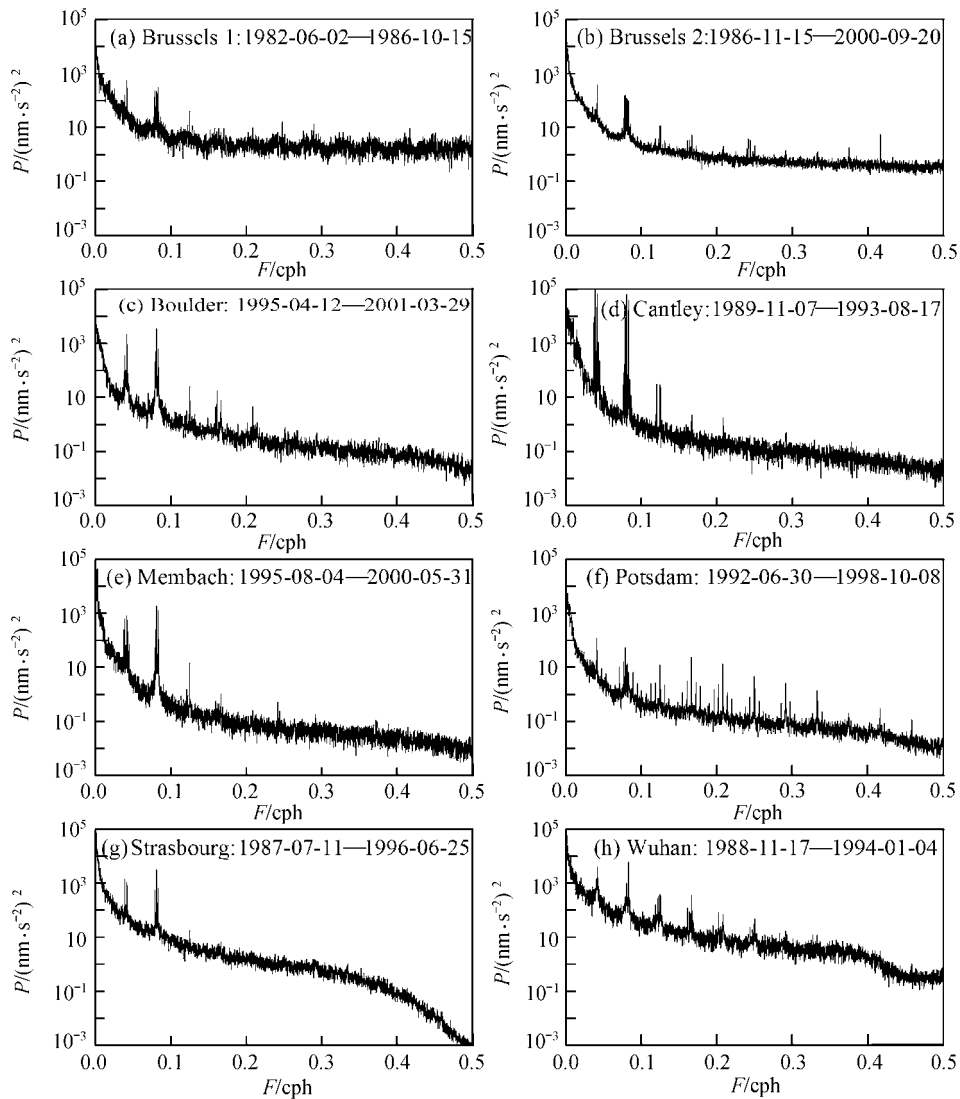


Fig. 3. Power spectral density for SG observation residuals in G-I group.

common spectral peaks are identified (marked as frequency as SP1, SP2, SP3, SP4, SP5, SP6, SP7 and SP8). The analysis shows that they are possible common weak harmonic signals relating to global movements, considering the use of effective stacking technique for global data and removing further effectively the remaining pressure influence. On the other hand, the PSD estimates for both pressure and gravity residuals in G-II at stations inside and outside Europe are also carried out, it is optimal that the similar peaks are situated. Therefore, referring to the theoretical computations given by Smith and Smylie, these common peaks can be inferred to the response of the geodynamical phenomenon of the translational oscillations of the ESIC.

In order to determine the oscillation parameters for these common spectral peaks, similar to Smylie, the reso-

nance near the common peaks is simulated by a harmonic oscillator given as^[6]

$$s(f) = \frac{A^2}{1 + 4[(f - f_0)/\Delta f]^2}, \quad (9)$$

where $s(f)$ is the PSD estimation at frequency f , A is resonant strength, f_0 the central frequency of the corresponding common peak, Δf is the length of the damping interval of the resonant frequency. Then the central period and quality factor can then be estimated by $T = 1/f_0$ and $Q = f_0/\Delta f$. By using a linear progressive iterative technique given by Marquadt for improving the numerical results, the resonant parameters (including the central frequency, resonant period, quality factor and resonant strength) for

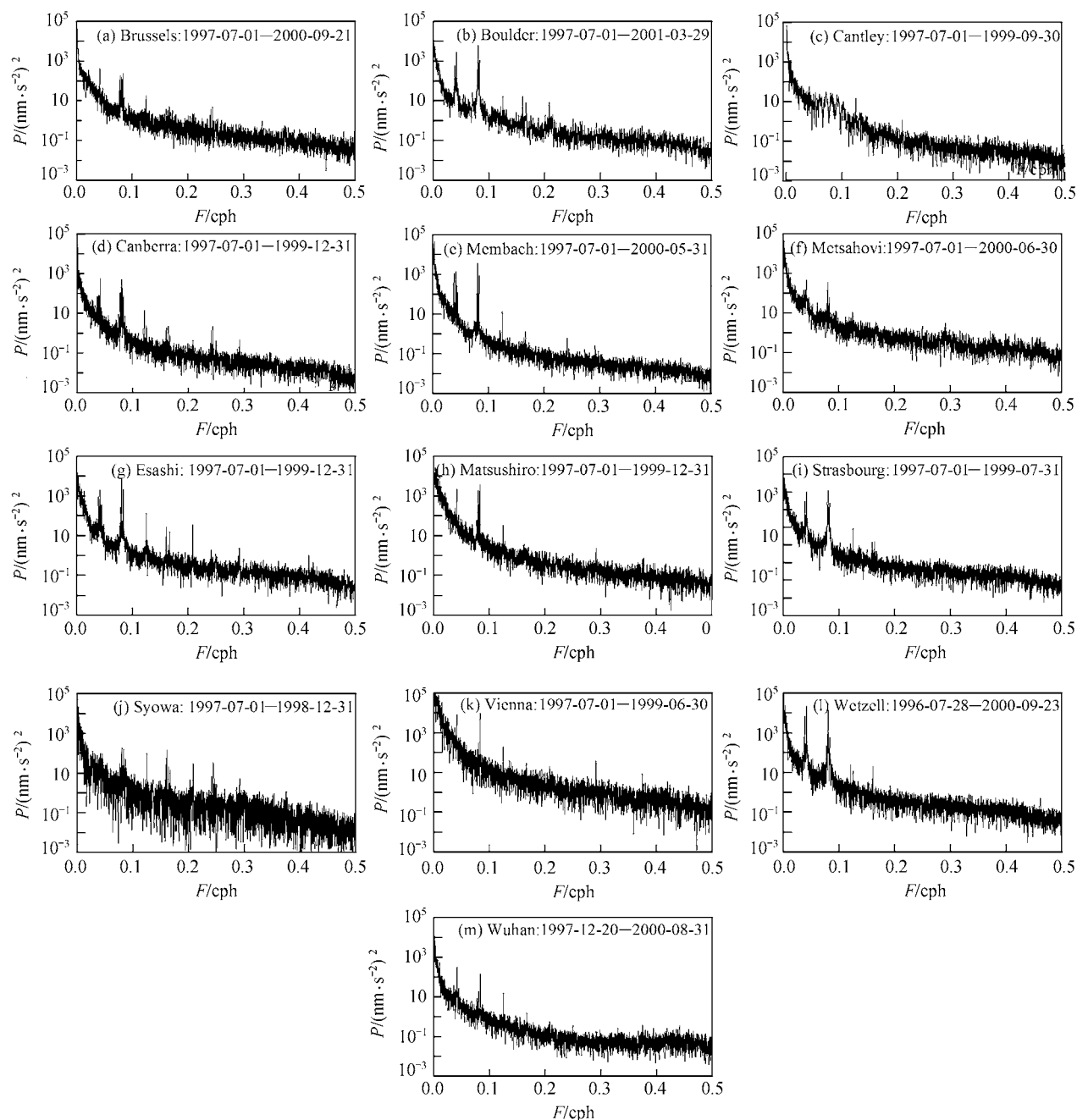


Fig. 4. Power spectral density for SG observation residuals in G-II group.

10 signals including 8 common peaks and 2 solar heating waves (S5 and S6) are calculated, and the results are given in Table 2.

It is indicated from comparison that the discrepancies of the resonant parameters between G-I and G-II groups are very small, then the mean of the results of two groups for each peak can be taken as the final ones. The numerical results show that the determined resonant periods

(4.93438 ± 0.00186 h, 4.42734 ± 0.001159 h and 4.09381 ± 0.00082 h) for SP1, SP4 and SP7, which correspond well with those of Slichter modes given in the theoretical computation by Smith using a generalized spherical harmonic expansion technique (4.916 h, 4.441 h and 4.055 h), the discrepancies are only 0.4%, -0.4% and 1.0%. This astonishing agreement between real detection and theoretical computation has temporal important meanings, it

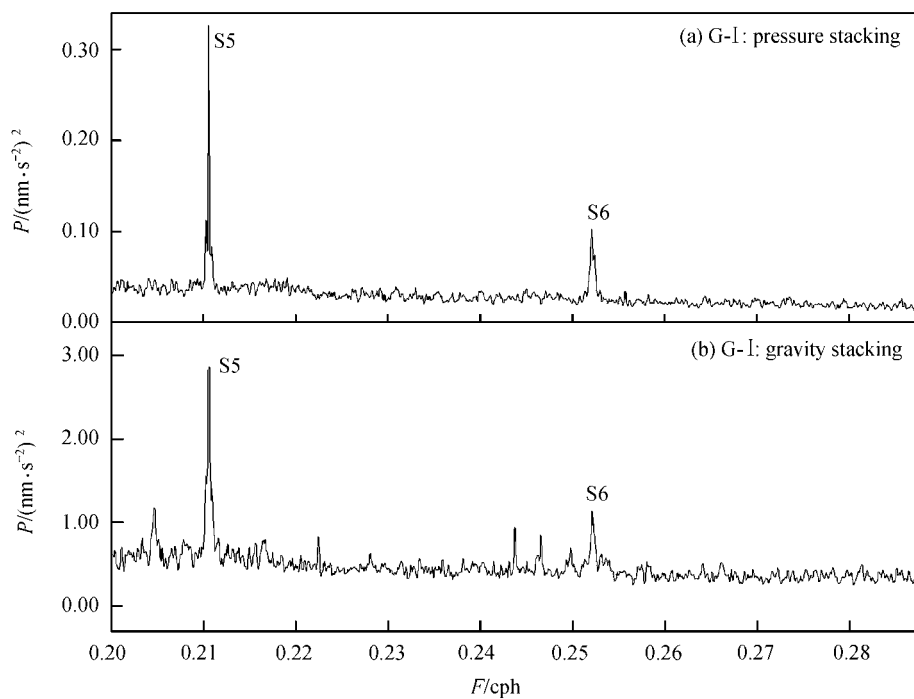


Fig. 5. Product spectral density in sub-tidal band in G- I group. (a) station pressure; (b) gravity residual.

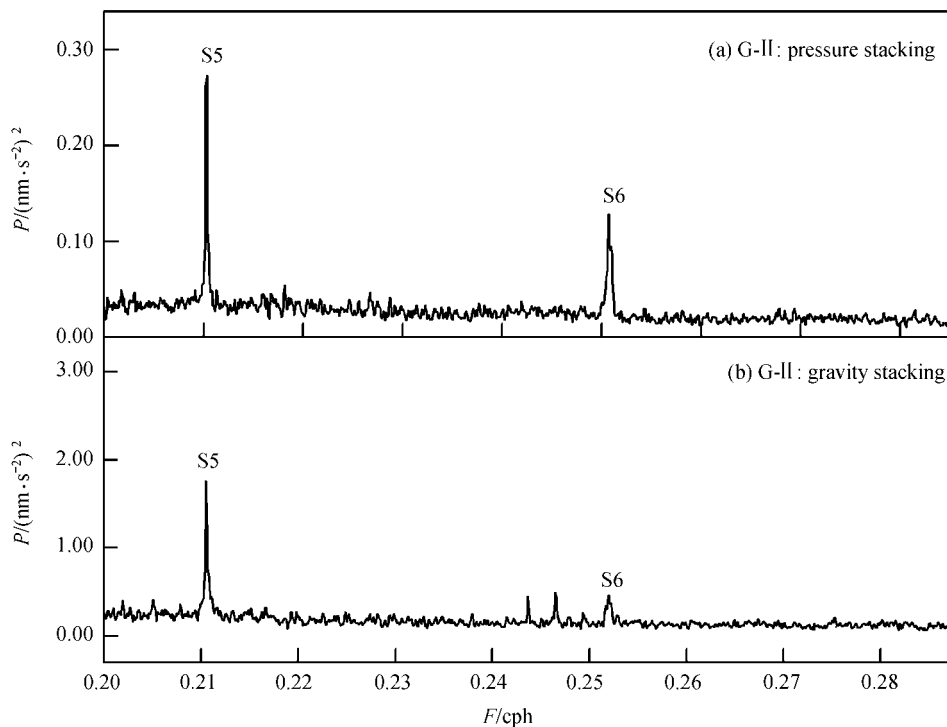


Fig. 6. Product spectral density in sub-tidal band in G- II group. (a) station pressure; (b) gravity residual.

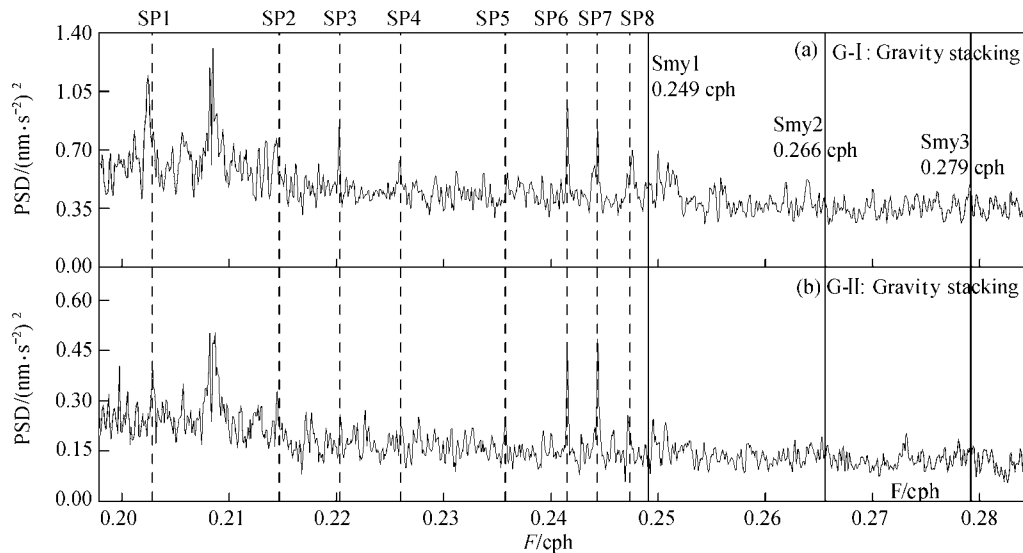


Fig. 7. Final PSD evaluation of the SG observations in sub-tidal band.

Table 2 Central frequency, eigen-period, quality factor and resonance strength for some common peaks

No.	$F(\text{cph})$	$P/T \cdot \text{h}^{-1}$	Q	ST
G-I group				
SP1	0.20244 ± 0.00009	4.93969 ± 0.00212	94 ± 14	0.98293 ± 0.02250
SP2	0.21435 ± 0.00003	4.66530 ± 0.00062	121 ± 10	0.87720 ± 0.00998
SP3	0.22021 ± 0.00017	4.54122 ± 0.00346	96 ± 46	0.75371 ± 0.03481
SP4	0.22592 ± 0.00005	4.42633 ± 0.00088	100 ± 13	0.74564 ± 0.01145
SP5	0.23608 ± 0.00020	4.23589 ± 0.00363	66 ± 20	0.68372 ± 0.01105
SP6	0.24154 ± 0.00007	4.14012 ± 0.00116	184 ± 41	0.81952 ± 0.04121
SP7	0.24421 ± 0.00006	4.09493 ± 0.00092	162 ± 29	0.81406 ± 0.02427
SP8	0.24755 ± 0.00004	4.03952 ± 0.00064	180 ± 32	0.78873 ± 0.01862
*S5	0.20833 ± 0.00003	4.80000 ± 0.00065	289 ± 33	1.68925 ± 0.06622
*S6	0.24998 ± 0.00006	4.00027 ± 0.00090	145 ± 20	0.93283 ± 0.03001
G-II group				
SP1	0.20288 ± 0.00007	4.92907 ± 0.00160	103 ± 19	0.56581 ± 0.01703
SP2	0.21451 ± 0.00007	4.66185 ± 0.00157	88 ± 17	0.51704 ± 0.01275
SP3	0.22034 ± 0.00014	4.53841 ± 0.00287	69 ± 25	0.43480 ± 0.01333
SP4	0.22582 ± 0.00012	4.42835 ± 0.00229	108 ± 31	0.44698 ± 0.01678
SP5	0.23574 ± 0.00007	4.24199 ± 0.00133	142 ± 33	0.42847 ± 0.01764
SP6	0.24153 ± 0.00007	4.14036 ± 0.00117	200 ± 42	0.52575 ± 0.03009
SP7	0.24434 ± 0.00004	4.09269 ± 0.00072	248 ± 35	0.59393 ± 0.02634
SP8	0.24722 ± 0.00007	4.04494 ± 0.00119	133 ± 25	0.43971 ± 0.01624
*S5	0.20835 ± 0.00003	4.79957 ± 0.00057	335 ± 39	1.14333 ± 0.04596
*S6	0.24987 ± 0.00004	4.00214 ± 0.00069	205 ± 26	0.62452 ± 0.02216

signifies that the 3 common peaks determined in our work correspond to the translational oscillations of the ESIC to be confirmed if the theoretical computation given by Smith is correct^[27]. The determined quality factors and resonant strengths can be also explained by using an

in-elasticity of the Earth's structure^[15].

On the other hand, the spectral splitting of the normal modes of the Earth's spheroidal oscillation can emerge due to the existence of the Earth's rotation and ellipticity^[28,29]. The analysis shows that a symmetric

property for SP6 and SP8 peaks at the two sides of SP7 exits. Two peaks at the symmetric place of SP1 in the PSD final results for G-II group (not yet marked) can be also found, though it is not obvious in the PSD final results for G-I group (may be covered by the noise). Therefore, the peaks at symmetric place of the SP1 and those at the symmetric place of the SP7 may correspond to the spectral splitting phenomenon due to the Earth's rotation and ellipticity, if the peaks of the SP1, SP4 and SP7 are caused by the normal modes of the ESIC.

4 Reliability test of the numerical results

In the ground surface gravity measurements, the weak signals of the translational oscillations of the ESIC are often covered by station background noise. Therefore it is still quite difficult for us to distinguish them by using the data from only unique station, even using high precision SG observations. Fortunately, the gravity signals induced by the translational oscillations of the ESIC are the global harmonic ones, therefore the global stacking technique can effectively reduce station background noise level, and enlarge relatively the common harmonic signals considering the various characteristics of the global station background noises. In order to check the reliability of the numerical computation during the determination of 8 common weak harmonic signals and also to know the detectable amplitude limitation of the global harmonic signals, the artificial weak harmonic signals with fix known frequency and various amplitudes are injected to each gravity residual series in G-II group. The power spectral densities for each series are calculated, and the final PSD estimation is then obtained. The numerical results show that when selecting frequency of the known harmonic signals as 0.23 cph, then (1) it is quite difficult for us to find the common peak in the final PSD estimation when injecting an artificial harmonic signal with an amplitude as of $5 \times 10^{-12} \text{ m/s}^2$, the injected signal is covered basically by station background noise; (2) there appears a weak common peak in the final PSD estimation when injecting an artificial harmonic signal with an amplitude as of $7 \times 10^{-12} \text{ m/s}^2$, the local signal-noise ratio arrives at 1.15, it signifies that the injected signal can be identified basically; and (3) there emerges an obvious common peak in the final PSD estimation when injecting an artificial harmonic signal with an amplitude as of $9 \times 10^{-12} \text{ m/s}^2$, the local signal-noise ratio arrives at 1.25, it means that the injected signal can be identified completely (Fig. 8). These tests have shown that the signal can be identified basically by using the PSD estimation, if there will be a global common harmonic signal with an amplitude of $7 \times 10^{-12} \text{ m/s}^2$. It proves also that the numerical results of 8 common peaks detected in this paper are reliable. Of course, except for 3 peaks among 8 are explained with theoretical modulation by Smith, the signal sources of the other peaks should be further studied.

5 Preliminary conclusions

By using 21 SG observation series at 21 stations in the GGP network, the Fourier power spectral densities and PSD estimations are carried out in this paper in order to identify the common signals relating to the translational oscillations of the ESIC after modifying the various error data and perturbation signals as well as removing of the theoretical tidal gravity signals. The numerical results show that the 8 common peaks are identified in the final PSD estimation for both G-I and G-II groups. The analysis demonstrates that the connection of the 8 peaks with station pressure and background noise is rejected, and the global weak harmonic signals induced by the geodynamics in the interior of the Earth are then confirmed. The resonant parameters for all peaks including the frequency, period, quality factor and resonant strength are determined accurately. The eigenperiods for 3 peaks among 8 correspond quite well with those of Slichter modes in theoretical prediction given by Smith, the discrepancy between them is only 0.4%, -0.4% and 1.0% respectively. This high agreement between practical identification and theoretical prediction signifies that the corresponding signals induced by the translational oscillations of the ESIC are confirmed. Some peaks can be explained by using the spectral splitting induced by Earth's rotation and ellipticity. Of course, no suitable reasons are found to explain other determined peaks, are they induced indeed by the ESIC? Or are they related to other geophysical and geodynamical factors as shallow sea tides and so on? The further checking should be developed in the forthcoming step.

On the other hand, it is necessary for us to declaim that the identification of the translational oscillations of the ESIC is still nowadays a difficult task since its weak signals on the ground based gravity measurements, therefore, it is also one of the world frontier projects in Earth sciences, our work is only a starting point and also a preliminary one. The main sophisticate points are given as (1) though the ideal laboratory accuracy of the SG measurement is at 10^{-11} m/s^2 level, the expected signals due to the translational oscillations of the ESIC are at the identical level, and also usually the real station background noise is much high; (2) the newest multistation stacking technique can overcome effectively the local background noise, relatively to enlarge the global weak harmonic signal, but its detection boundary amplitude of the harmonic signal is at $7 \times 10^{-12} \text{ m/s}^2$ that is at the same level with SG lab precision; (3) there is no one confidential theoretical model of the translational oscillations of the ESIC to be recognized by international colleague for the real detection reference; and (4) the mechanical sources of the translational oscillations of the ESIC are not yet clear until now, are they induced really by large earthquakes in deep interior of the Earth? or by the strong electronic-magnetic spiral field induced

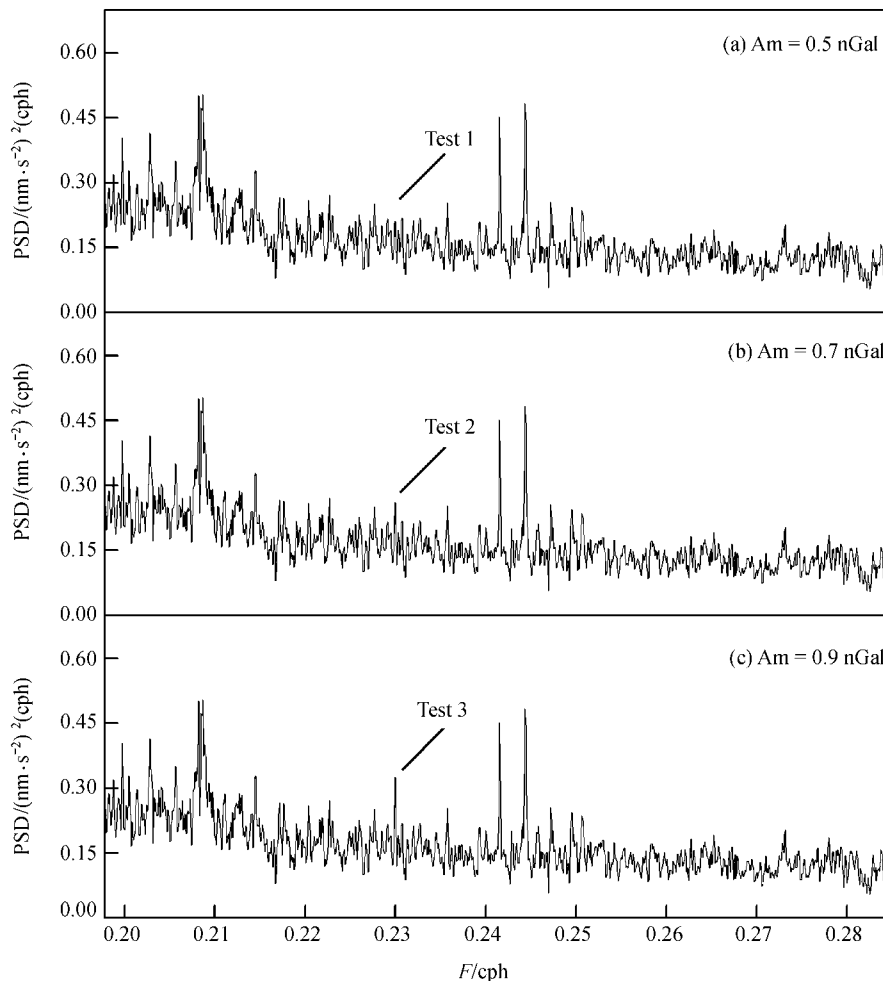


Fig. 8. Final PSD estimation when injecting an artificial weak harmonic signal.

by the iron components and high temperature in the liquid outer core and together with topography coupling force torques at the inner core and outer core boundaries due to the Earth's rotation? Therefore the deep study and reliable conclusions will depend on the confidential theoretical model, the accumulating global long period high precision SG observations and the detailed data preprocessing works for improving the resolution of the gravity signals.

Acknowledgements Authors are grateful to Crossley, the GGP Chairman from St. Luis University, USA and all station managers for collecting high quality SG data. Sun Heping thanks Smylie for providing support to visit York University, Canada and also for providing parts of computing codes. Vandercoilden, L. and Hendrickx, M. from the GGP center in Royal Observatory of Belgium took part in the data arrangement and preprocessing. This work was supported jointly by the Key Project of the Knowledge Innovation of the Chinese Academy of Sciences (Grant No. KZCX3-SW-131), the Key International Scientific Cooperation Project via the Ministry of Science and Technology of China (Grant No. 2002CB713904) and the National Natural Science Foundation of China (Grant Nos. 40174022 and 40374029).

References

1. Smith, M. L., Translational inner core oscillations of for a rotating, slightly elliptical Earth, *Journal of Geophysical Research*, 1976, 81(17): 3055—3064.
2. Smylie, D. E., Rochester, M. G., Compressibility, core dynamics and the subseismic wave equation, *Physics of the Earth and Planetary Interior*, 1981, 24: 308—319. [\[DOI\]](#)
3. Crossley, D., Hinderer, J., Casula, G. et al., Network of superconducting gravimeters benefits a number of disciplines, *Eos, Transactions, American Geophysical Union*, 1999, 80(11), 121: 125—126.
4. Melchior, P., Ducarme, B., Detection of inertial gravity oscillations in the earth's core with a superconducting gravimeter at Brussels, *Physics of the Earth and Planetary Interior*, 1986, 42: 129—134. [\[DOI\]](#)
5. Smylie, D. E., The inner core translational triplet and the density near the Earth's center, *Science*, 1992, 255: 1678—1682.

ARTICLES

6. Smylie, D. E., Viscosity near Earth's solid inner core, *Science*, 1999, 284: 461—463. [\[DOI\]](#)
7. Slichter, L. B., The fundamental free mode of the Earth's inner core, *Natl. Acad. Science*, 1961, 47: 186—190.
8. Smith, M. L., Translational inner core oscillations of for a rotating, slightly elliptical Earth, *Journal of Geophysical Research*, 1976, 81(17): 3055—3064.
9. Hinderer, J., Crossley, D. J., Jensen, O., A search for the Slichter triplet in superconducting gravimeter data, *Physics of the Earth and Planetary Interior*, 1995, 90: 183—195. [\[DOI\]](#)
10. Cummins, P., Wahr, J., Agnew, D. et al., Constraining core undertones using stacked IDA gravity records, *Geophysical Journal International*, 1991, 106: 189—198.
11. Smylie, D. E., Hinderer, J., Richter, B. et al., The product spectra of gravity and barometric pressure in Europe, *Physics of the Earth and Planetary Interior*, 1993, 80: 135—157. [\[DOI\]](#)
12. Courtier, N., Ducarme, B., Goodkind, J. et al., Global Superconducting gravimeter observations and the search for the translational modes of the inner core, *Physics of the Earth and Planetary Interiors*, 2000, 117: 3—20. [\[DOI\]](#)
13. Sun, H. P., Ducarme, B., Xu, J. Q., Preliminary results of the free core nutation eigenperiod obtained by stacking SG observations at GGP stations, *Bulletin D'Information Marées Terrestres*, 2002, 136: 10725—10728.
14. Xu, J. Q., Sun, H. P., Luo, S. C., Study of the Earth's free core nutation by tidal gravity data recorded with international superconducting gravimeters, *Science in China, Series D*, 2002, 45(4): 337—347. [\[Abstract\]](#) [\[PDF\]](#)
15. Sun, H. P., Xu, J. Q., Ducarme, B., Experimental earth tidal models in considering nearly diurnal free wobble of the Earth's liquid core, *Chinese Science Bulletin*, 2003, 48(9): 935—940. [\[Abstract\]](#) [\[PDF\]](#)
16. Goodkind, J. M., The superconducting gravimeters principals of operation, current performance and future prospects, *Proc. workshop on non-tidal gravity changes* (ed. Poitevin, C.), Luxembourg: Conseil de L'Europe Cahiers du Centre Européen de Géodynamique et de Séismologie, 1991, 9: 81—90.
17. Ducarme, B., Sun, H. P., Tidal gravity results from GGP network in connection with tidal loading and earth response, *Journal of the Geodetic Society of Japan*, 2001, 47(1): 308—315.
18. Ducarme, B., Sun, H. P., Xu, J. Q., New Investigation of Tidal Gravity Results from the GGP Network, *Bulletin D'Information Marées Terrestres*, 2002, 136: 10761—10775.
19. Vauterin, P., Tsoft: Graphical and interactive software for the analysis of Earth tide data, *Proc. 13th Int. Sympos. Earth Tides* (eds. Paquet, P., Ducarme. B.), Brussels: Royal Observatory of Belgium, 1998. 481—486.
20. Merriam, J. B., The atmospheric pressure correction in gravity at Cantley, Quebec, *Proc. 12th Int. Sympos. Earth Tides* (ed. Hsu, H. T.), Beijing: Science Press, 1993. 161—186.
21. Sun, H. P., Hsu, H. T., Jentzsch, G. et al. Tidal gravity observations obtained with superconducting gravimeter and its application to geodynamics at Wuhan/China, *Journal of Geodynamics*, 2002, 33(1-2): 187—198. [\[DOI\]](#).
22. Tamura, Y., A harmonic development of the tide-generating potential, *Bulletin D'Information Marées Terrestres*, 1987, 99: 6813—6855.
23. Wenzel, H. G., Earth tide data processing package ETERNA 3.30: the nGal software, *Proc. 13th Int. Sympos. Earth Tides* (eds. Paquet, P., Ducarme. B.), Brussels: Royal Observatory of Belgium, 1998. 487—494.
24. Sun, H. P., Luo, S. C., Theoretical computation and detection of the atmospheric gravity signals, *Chinese Journal of Geophysics*, 1999, 41(3): 405—413.
25. Sun, H. P., Comprehensive researches for the effect of the ocean loading on gravity observations in the Western Pacific Area, *Bulletin D'Information Marées Terrestres*, 1992, 113: 8271—8292.
26. Venedikov, A. P., Vieira, R., de Toro, C., On the determination of the D and SD Earth tides generated by the tidal potential of the third order, *Bulletin D'Information Marées Terrestres*, 1976, 126: 9635—9637.
27. Sun, H. P., Xu, J. Q., Ducarme, B., Search for the Translational Triplet of the Earth's Solid Inner Core by SG Observations at GGP Stations, *Bulletin D'Information Marées Terrestres*, 2003, 138: 10977—10985.
28. Dahlen, F. A., The normal modes of a rotating, elliptical Earth, *Geophys. J. Roy. Astron. Soc.*, 1968, 16: 329—367.
29. Dahlen, F. A., The normal modes of a rotating, elliptical Earth-II Near-resonance multiplet coupling, *Geophys. J. Roy. Astron. Soc.*, 1969, 18: 397—436.

(Received May 15, 2003; accepted March 1, 2004)